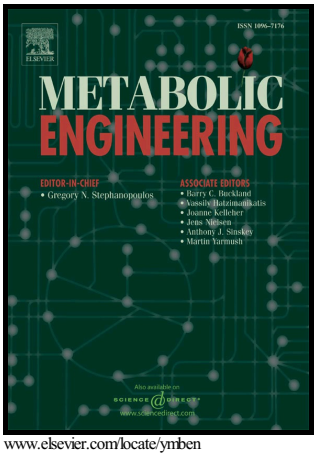

www.elsevier.com/locate/ymben

Intermediate-sensor assisted push-pull strategy and its application in heterologous deoxyviolacein production in *Escherichia coli*

Mingyue Fang, Tianmin Wang, Chong Zhang, Jili Bai, Xiang Zheng, Xuejin Zhao, Chunbo Lou, Xin-Hui Xing

PII: S1096-7176(15)00134-2
DOI: http://dx.doi.org/10.1016/j.ymben.2015.10.006
Reference: YMBEN1056

To appear in: *Metabolic Engineering*

Received date: 22 August 2015
Revised date: 22 September 2015
Accepted date: 15 October 2015

Cite this article as: Mingyue Fang, Tianmin Wang, Chong Zhang, Jili Bai, Xiang Zheng, Xuejin Zhao, Chunbo Lou and Xin-Hui Xing, Intermediate-sensor assisted push-pull strategy and its application in heterologous deoxyviolacein production in *Escherichia coli*, *Metabolic Engineering* http://dx.doi.org/10.1016/j.ymben.2015.10.006

Manuscript

Intermediate-sensor assisted push-pull strategy and its application in heterologous deoxyviolacein production in *Escherichia coli*

Mingyue Fang[1]*, Tianmin Wang[1]*, Chong Zhang[1#], Jili Bai[1], Xiang Zheng[1], Xuejin Zhao[2], Chunbo Lou[2], and Xin-Hui Xing[1]

[1]Key Laboratory for Industrial Biocatalysis, Ministry of Education, Institute of Biochemical Engineering, Department of Chemical Engineering, Tsinghua University, Beijing, China, 10084

[2]Institute of Microbiology, Chinese Academy of Science, Beijing 10084, China

*These authors contributed equally to this work

[#]Corresponding authors

Chong Zhang

E-mail: chongzhang@tsinghua.edu.cn, Fax: +86-10-62794771

Abstract

Because high-throughput screening tools are typically unavailable when using the pathway-engineering approach, we developed a new strategy, named intermediate sensor–assisted push-pull strategy, which enables sequential pathway optimization by incorporating a biosensor targeting a key pathway intermediate. As proof of concept, we constructed an L-Trp biosensor and used it to optimize the deoxyviolacein biosynthetic pathway, which we divided into two modules with L-Trp being the product of the upstream and the substrate of the downstream module for deoxyviolacein synthesis. Using the biosensor and fluorescence-activated cell sorting, the activities of the two modules were sequentially and independently optimized in *Escherichia coli* to achieve the desired phenotypes. By this means, we increased the deoxyviolacein titer 4.4-fold (1.92 g/L), which represents the greatest deoxyviolacein production reported. This work suggests that a biosynthetic pathway can be enhanced to produce a value-added secondary metabolite(s) without available end-product screening method by using a central metabolic junction molecule biosensor(s).

Key words:

Pathway engineering, High-throughput screening, Biosensor, Deoxyviolacein biosynthesis, Sequential optimization

1. Introduction

Microbial production of bulk commodities or value-added metabolites presents as an attractive, sustainable, and green industrial solution. By mutating an endogenous gene(s) and introducing a heterologous pathway(s), the metabolic network in a host microbe can be improved for production of the desired molecule(s) (Ajikumar et al., 2010; Atsumi et al., 2008; Ro et al., 2006). However, to achieve industrial level productivity (Jones et al., 2015; Woolston et al., 2013), efforts that fine-tune the metabolic flux in the engineered pathway(s) are often required. Early efforts to engineer microbial factories focused on individually manipulating one or several units in the microbial machinery, i.e., knocking out a competing pathway or overexpressing a key enzyme(s), with the assumption that multiple modifications would be additive (Yuan et al., 2006). Although moderate productivity increases were achieved, this approach generally suffers from the limited phenotype space explored, and metabolic flux imbalance can often be a severe problem owing to such side effects as the accumulation of a toxic intermediate(s) and/or negative feedback, which would decrease the target product yield (Chen et al., 2011; Paddon et al., 2013). As a solution, combinatorial approaches simultaneously covering multiple targets within a pathway offer an opportunity to systematically sample a wider area of phenotype space (Zelcbuch et al., 2013). Multivariate modular metabolic engineering (Biggs et al., 2014), a focused combinatorial approach, groups pathway enzymes as modules so that expression of the enzymes within the module(s) can be varied simultaneously by just a single genetic manipulation. This technique has proven to be a powerful tool as it can potentially cover a wider range of phenotype space using only a small number of modular constructs. An equally important advance is regression modeling that is used to predict the pathway flux landscape based on only a small number of measurements

(Lee et al., 2013). Both of these approaches negate the need for exhaustive genotype screening and have achieved substantial microbial cell factory optimizations (Ajikumar et al., 2010; Lin et al., 2014a; Wu et al., 2013; Xu et al., 2013). However, these strategies still retrieve suboptimal solutions within the surveyed phenotype space because modular structure design is an artificial construct and more complex pathway architectures always involve more complicated phenotype landscapes (Zelcbuch et al., 2013), which dramatically increases screening requirements.

Given the development of more powerful library construction methods, e.g., clustered regularly interspaced short palindromic repeats (CRISPR)/CRISPR-associated proteins (Cas) (Jiang et al., 2013; Wiedenheft et al., 2012), multiplexed automated genome engineering (Wang et al., 2009), and oligo-linker-mediated assembly (OLMA method; S. Zhang *et al.*, submitted) that uses Golden Gate shuffling (Engler et al., 2009)), we can now construct complex combinatorial genotype libraries of high quality, thus significantly expanding the available genotype space. Incorporating various genotype-generating techniques into pathway engineering enables a more exhaustive exploration of phenotype space and, consequently, the potential to recover better-optimized strains. However, such genotype-generating techniques also required a much stronger screening method(s), which can quickly out-strip the throughput speed of current analytical methods. Biosensor-driven pathway optimization has been coupled with fluorescence-activated cell sorting (FACS) (Binder et al., 2013), or lethal selection (Yang et al., 2013), to meet this screening challenge and has achieved enhanced microbial production of many chemicals, e.g., L-Met (Mustafi et al., 2012), 1-butanol (Dietrich et al., 2013), L-Lys (Binder et al., 2013; Yang et al., 2013), triacetic acid lactone (Tang et al., 2013), and naringenin (Raman et al., 2014a). However, currently, despite several successful examples (Chen

et al., 2015; Tang and Cirino, 2011; Tang et al., 2013, 2008; Yang et al., 2013), because *de novo* design of biosensors is difficult, the number of biosensors for the metabolic molecules is still very limited, and most have been designed based on a naturally occurring regulatory system, e.g., a transcription factor or riboswitch (Dietrich et al., 2013; Raman et al., 2014a; Siedler et al., 2014). In addition, because our knowledge of secondary metabolic pathway regulation is very incomplete, even when value-added molecule targets are produced from such pathways, if an associated transcription factor or riboswitch has not been identified, a biosensor for the target products is very hard to be developed. Conversely, it should be much easier to develop biosensors for metabolites found in central carbon pathways, e.g., amino acid (Cho et al., 2012) or fatty acid (Zhang et al., 2012) biosynthetic pathways, because their regulatory mechanisms have been intensively studied.

One potential but rarely explored strategy that would allow for industrial production of secondary metabolites, is to use a biosensor that responds to a molecule produced in a central carbon pathway and that is a precursor for the target secondary metabolite pathway(s). We, therefore, propose a strategy, named intermediate sensor–assisted push-pull strategy (InterSPPS), that uses a biosensor for a central pathway intermediate to balance upstream and downstream modular pathway flux in a sequential push-pull manner so as to overproduce a target secondary metabolite. By monitoring the biosensor response for an intermediate joining two modules in a pathway, the upstream module can first be enhanced by a metabolic push reported as an increased biosensor signal in the absence of the downstream module. Subsequently, the downstream module can be enhanced as a metabolic pull, reflected by the decreased reporting signal of the biosensor owing to the depletion of the accumulated intermediate (Fig. 1a). As a proof-of-concept, we chose the microbial synthesis of

deoxyviolacein (Fig. 1b), a secondary metabolite with a variety of bioactivities (Jiang et al., 2012; Wang et al., 2012). Because L-Trp is the key intermediate in the biosynthesis of deoxyviolacein from glucose (Yang et al., 2011), we first engineered an L-Trp biosensor based on the leader-peptide mechanism (encoded in *tnaC*) that regulates transcription of the *tnaCAB* operon induced by L-Trp (Gong and Yanofsky, 2002). We then combinatorially optimized the L-Trp biosynthetic pathway in *Escherichia coli* to increase L-Trp accumulation, and the clone with the greatest accumulation of L-Trp (100-fold increase) was identified by FACS screening. Subsequently, a deoxyviolacein pathway library was constructed based on the mutation of its key**,** rate-limiting enzyme VioB and coupled to the optimized L-Trp biosynthesis pathway. The strain with the most improved deoxyviolacein production owing to the combined, balanced pathway was retrieved based on the decreased L-Trp biosensor signal relative to the bulk population (Fig. S1).

By using our InterSPPS approach, we successfully increased deoxyviolacein biosynthesis via fed-batch fermentation to a titer of 1.92 g/L and a productivity of 40 mg/L/h, which represents the greatest production of deoxyviolacein reported to date that does not need addition of L-Trp into the fermentation medium. This work demonstrates that a biosynthetic pathway can be engineered in a high-throughput manner without available end-product screening method by using one or more central metabolic junction molecule biosensors to produce bioactive and value-added secondary metabolites.

2. Materials and Methods

2.1. Strains and culture conditions

Strains and plasmids used in this work are listed in Table 1. For L-Trp and deoxyviolacein fermentations, single colonies were each inoculated into 10 mL LB broth in a 50 mL flask and cultured overnight at 37°C. Then 5% (v/v) of the seed culture was added into 20 mL of M9-YE medium (10 g/L glucose) (Ye et al., 2009) in a 100 mL flask and cultivated at 37°C until the culture OD_{600} was between 0.8 and 1.0 (~3 h). Next, after adding isopropyl-thio-β-D-galactopyranoside (IPTG; final concentration, 24 mg/L), the temperature was held at 28°C for 24 h for L-Trp production or at 20°C for 48 h for deoxyviolacein production. The OD_{600} values of the cultures were measured using an Amersham Bioscience spectrophotometer. The culture media also contained 100 mg/L ampicillin, 50 mg/L kanamycin, 34 mg/L chloromycetin, and/or 10 mg/L tetracycline as needed to maintain the presence of a plasmid(s).

2.2. General description of plasmid construction

Primer sequences are listed in Table S1. General information concerning plasmid construction is described immediately below. All cloning procedures were performed according to the manufacturers' instructions. DNA purification and isolation of high quality plasmids used reagents from Omegta Bio-Tek kits. *E. coli* K12 MG1655 and BL21(DE3) genomic DNAs were purified using reagents from Tiangen Biotech kits. DNA restriction and amplification enzymes were from New

England Biolabs. During plasmid construction, unless otherwise specified, *E. coli* DH5a (BioMed) served as the host and was cultured in Luria-Bertani (LB) broth or on LB-containing agar plates at 37°C.

2.3. Construction of pSentrp

The plasmid pSentrp contains the gene for the L-Trp biosensor, which is composed of *eGFP* (PCR-amplified using the primers Sentrp-2-F and –R from the plasmid pHygEGFP (Clontech)) fused downstream to the *tnaCAB* operon regulatory element *tnaC* (PCR-amplified from *E. coli* K12 MG1655 genomic DNA with Sentrp-1-F and -R primers; 24-bp upstream of *tnaC* to 30-bp downstream of the *tnaA* start codon, RefSeq: NC_000913.3, 3,888,411-3,888,759, (Liu et al., 2011); Fig. S2). The amplified and purified DNAs were ligated into *Nco*I/*Hind*III-digested pTrc99A to construct pSentrp. By this means, *tnaC* acts as the input monitor dependent on the intracellular L-Trp concentration and converts the concentration into an EGFP fluorescence-monitoring signal.

2.4. Construction of the plasmid library Trp-Push by OLMA method

In general, the procedure described below followed the protocol for OLMA pathway engineering (S. Zhang *et al.*, submitted) (Detailed protocol can be found in the supplementary materials for OLMA). Briefly, the open reading frames for *serA* and *aroG* were amplified from *E. coli* BL21(DE3) genomic DNA, with primers that introduced a site mutation(s) ($SerA^{fbr}$: Thr327Asp, ACT to GAT(Rodrigues et al., 2013) and $aroG^{fbr}$: Asp146Asn, GAT to AAT and Pro150Leu, CCA to CTA (Kikuchi

et al., 1997)) so as to prevent feedback inhibition to these enzymes. *trpE*^{fbr}*D* (Met293Thr, ATG to ACG and Ser40Phe, TCC to TTC) (Spraggon et al., 2001) was amplified from pED (Fang et al., 2015). Purified *trpE*^{fbr}*D*, *SerA*^{fbr}, and *aroG*^{fbr} were individually ligated into a linearised pHD (Life Technology) at the *Bsa*I restriction site, to construct pHD-trpED, pHD-serA, and pHD-aroG, respectively. The acceptor vector pACYCDuet was also PCR-amplified using the primers pACYCDuet-F and -R to contain a *Bsa*I site.

We used an RBS calculator (Salis et al., 2009) to determine the theoretical expression rates of *trpE*^{fbr}*D*, *SerA*^{fbr}, and *aroG*^{fbr} when under the control of various RBS sequences. 10 (*SerA*^{fbr}, and *aroG*^{fbr}) or 15 (*trpE*^{fbr}*D*) RBS sequences were selected so that the largest possible range of translation initiation rates would be covered (Table S2). The DNAs in the RBS library (synthesized by Invitrogen) were single stranded and flanked with *Bsa*I sites. An annealing process was carried out for each pair of RBS oligomers to generate double stranded DNAs with an appropriate adapter site. All double-stranded RBS fragments were treated with T4 polynucleotide kinase (New England Biolabs) prior to OLMA.

We used OLMA method to construct the Trp-Push library. Plasmids carrying *trpE*^{fbr}*D*, *SerA*^{fbr} and *aroG*^{fbr} (pHD-trpED, pHD-SerA, and pHD-aroG), adaptable double-stranded RBS sequences, and pACYCDuet were assembled in a single restriction-ligation step with *Bsa*I and ligase (New England BioLabs). Next, the ligated DNA was treated with Plasmid-Safe ATP-Dependent DNase (Epicentre) followed by transformation into chemically competent JM109 cells (Biomed). Sanger sequencing of plasmids from 10 colonies confirmed the reliability of the library.

2.5. Generation of the error-prone vioB library, Vio-Pull

The following OLMA procedure was performed to create the Vio-Pull library containing *vioB* mutants and the other deoxyviolacein pathway genes. Plasmid pDvio carrying the deoxyviolacein biosynthetic cluster was constructed by transferring the deoxyviolacein biosynthetic pathway *vioABEC* from pComVioΔD (Jiang et al., 2012) into doubly digested pRSFDuet using the primers BglII-vioA-F and XhoI-vioE-R (The *vioABCDE* cluster was originally isolated and cloned from *Duganella* sp. B2, GenBank accession number GQ266676, Fig. S3) (Jiang et al., 2010). Subsequently, *vioA* (the *Bsa*I site within the original sequence had been removed (C453T, synonymous mutation) and *vioCE* were individually amplified from pDvio and Gibson assembled in pHD to generate pHD-vioA and pHD-vioCE, respectively. The fragment of *vioB* was amplified using error prone PCR (Zhao et al., 1999) and purified as linear fragments. pRSFDuet was converted into an improved OLMA acceptor vector. Briefly, the synthetic template (Fig. S4, SynGenTech) was used to remove the pRSFDuet *Bas*I site and introduce two closely located *Bsa*I sites for OLMA. This fragment was amplified using the primers pRSF-part-F and -R and then ligated into a *Bsa*I/*Nde*I doubly digested pRSF-Duet by Gibson assembly to yield pRSF-Duet-BsaI. pHD-vioA, pHD-vioCE, the *vioB* mutant library, and the linear acceptor pRSF-Duet-BsaI were assembled by OLMA method as described above for the Trp-Push library to generate the Vio-Pull library. The reliability of the library was confirmed by the purple appearance after transformation and subsequent cultivation of its clones at 20°C for 48 h.

2.6. Quantification of extra- and intracellular L-Trp

To quantify extracellular L-Trp, fermentation samples were centrifuged at 13000 × *g* for 5 min, and 10 μL of each supernatant was then individually injected into an Inertsil ODS-SP 4.6 × 250 mm column heated at 40°C controlled by a Shimadzu HPLC system equipped with a UV detector set to 280 nm. The eluents were methanol (A) and 0.05% (w/v) aqueous H_3PO_4. The elution system was 2% A between 0 and 3 min; a linear gradient of 2% to 80% A between 3 and 30 min; 80% A between 30 and 40 min; a linear gradient of 80% to 2% A between 40 and 50 min; and 2% A between 50 and 60 min, all at a flow rate of 0.5 mL/min. The standard curve used for L-Trp (Sigma-Aldrich) quantification is shown in Fig. S5a. To quantify the intracellular L-Trp concentration, L-Trp in the cells was extracted by silicone oil centrifugation according to Klingenberg, *et al.* (Klingenberg and Praff, 1967) and the details were described in the supplementary materials.

2.7. Effectiveness of the biosensor characterized by fluorescence intensity

Overnight LB cultures (0.5 mL) of cells containing pSentrp were individually incubated in 10 mL of M9-YE medium in 50 mL flasks, and when the culture OD_{600} were ~0.6, IPTG (final concentration, 24 mg/L) was added to induce expression of the biosensor. Subsequently, cells were concentrated by centrifugation to an OD_{600} of 2 to 4 in MOPS minimal medium containing 4% (w/v) glucose (Neidhardt et al., 1974). Briefly, each culture was washed three times to remove the LB broth, and finally, each culture was concentrated by around 5-fold. Various amounts of Ala-Trp were then

added into individual culture samples to control the intracellular L-Trp concentration. Furthermore, after a 4-h incubation, cells were subjected to fluorescence analysis.

For flow cytometry, each culture was first diluted 400-fold with a PBS-type buffer (8.0 g/L NaCl, 0.2 g/L KCl, 1.42 g/L Na_2HPO_4, 0.24 g/L KH_2PO_4, pH 7.4) and then analysed using a FACSCalibur flow cytometer (BD Biosciences). The excitation wavelength was 488 nm, and the emission wavelength was 530 nm. Data from 50,000 events were collected for each sample, and non-bacterial particles were excluded by electronic gating. The fluorescence gain was adjusted for the fluorescence intensity of bacteria containing an empty pTrc99a vector. Data were processed using BDFACSDiva software (BD Bioscience) and medium fluorescence unit (MFU) was calculated for each population.

For fluorescence spectrometry, aliquots of cell suspensions were diluted five-fold in the PBS-type buffer described in the preceding paragraph, and fluorescence was measured with an F-2500 Hitachi Fluorescence Reader (excitation wavelength, 488 nm; emission wavelength, 510 nm) and relative fluorescence unit (RFU) was obtained. Fluorescence was further normalised to the culture OD_{600} value.

The FACS protocol was the same as flow cytometry analysis except that an FACS Aria flow cytometer (BD Biosciences) was used.

2.8. Quantification of deoxyviolacein

After fermentation, cells were pelleted by centrifugation at 13000 × *g* for 5 min and then extracted in ethanol with sonication. After a nearly complete extraction (the pellet showed no purple coloration by eyesight), the sample was centrifuged again, and the absorbance at 568nm of the supernatant was determined to measure the

deoxyviolacein concentration (the standard deoxyviolacein curve is shown in Fig. S5b). The cell mass was determined using the OD_{600} of the re-suspended pellet (Jiang et al., 2010; Yang et al., 2011).

2.9. Fed-batch fermentation in a bioreactor

A 5-L, stirred-tank bioreactor (Applicon) was used, as was modified M9-YE medium (20 g/L glucose, 3 g/L KH_2PO_4, 0.5 g/L NaCl, 1 g/L NH_4Cl, 5 g/L yeast extract, 5 g/L tryptone, 1 mM $MgSO_4$, and 0.1 mM $CaCl_2$). A seed culture was prepared by inoculating one colony of B8/pTrpH1/pDVio-L1 into a 500 mL flask containing 100 mL of culture medium. The culture was incubated at 37°C and 200 rpm for 16 h and then transferred into the bioreactor containing 2 L of medium. Fermentation was first performed at 37°C for 3 h to allow for biomass accumulation, and then the temperature was lowered to 20°C at which time IPTG (final concentration, 24 mg/L) was added. A 25% dissolved O_2 concentration and a pH of 7.0 were maintained by an Inpro 6800/12/320 O_2 sensor (Mettler Toledo) and a 405-DPAS-SC-K8S/325 pH electrode in conjunction with a 10 M ammonia titration, respectively. During fermentation, after 20 h of incubation, the glucose concentration was measured by the dinitrosalicylic acid method (Miller, 1959) and subsequently maintained at ~10 g/L by manual addition of glucose. The samples were withdrawn periodically to determine the deoxyviolacein concentration and cell density (OD_{600}) as described in the last section.

2.10. Statistical Analysis

Statistical analysis was performed using the two-tailed Student's *t*-test. Results are given as the mean ($n \geq 3$) ± the standard deviation (SD). Differences in values are considered significant when $P < 0.05$.

3. Results

3.1. Construction and characterisation of the L-Trp biosensor

Biosensors for L-Met (Mustafi et al., 2012), L-Lys (Binder et al., 2012; Yang et al., 2013), L-Val (Mustafi et al., 2014), and L-Arg (Schendzielorz et al., 2014) have been constructed based on their well-studied, naturally occurring biosynthetic pathways and regulatory mechanisms (Cho et al., 2012; Cipriano et al., 2013). Given these successes, by analogy, we constructed pSentrp (Fig. 2a) that encodes an L-Trp biosensor. The biosensor is composed of *tnaC*—which encodes the leader sequence of the *tnaCAB* operon (for which its expression is induced by L-Trp (Gong and Yanofsky, 2001; Yanofsky et al., 1991))—fused upstream to the gene for the enhanced green fluorescence protein (EGFP) (Fig. 2a).

To test the performance of this biosensor, we induced *eGFP* expression by adding Ala-Trp to the culture medium, with Ala-Trp dipeptide controlling the intracellular L-Trp concentration(Binder et al., 2012), or by internal accumulation of L-Trp. For the Ala-Trp trial, *E. coli* BL21(DE3) containing pSentrp was used. The maximum intracellular L-Trp concentration was detected at 1.5 h after addition of 1.5 mM Ala-Trp (Fig. S6). The intracellular L-Trp concentration was linearly dependent on the extracellular dipeptide concentration (Fig. S7). At 4 h after the dipeptide addition (2~3 h needed for sufficient EGFP expression), EGFP fluorescence was measured by flow cytometry and fluorescence spectrometry. The dipeptide-

fluorescence signal dose curve represented sigmoid shape with detection limit ranging from 0.1mM (measured by fluorescence spectrometry, Fig. S8a) up to 1.5 mM dipeptide (The fluorescence signal plateaued when the dipeptide concentration exceeded 1.5 mM even though more intracellular L-Trp accumulated at greater Ala-Trp concentrations). The linear response range of this sensor is shown in Figure 2b and therefore, representing an ~8-fold dynamic range. Finally, the specificity of the biosensor was confirmed as the aromatic amino acids, L-Tyr and L-Phe, induced only a small, respectively no fluorescence signal (Fig. S8b).

We next tested the performance of the biosensor in genetically modified strains of the L-Trp-producing *E. coli* B8/pED (Fang et al., 2015) that overexpresses *trpE*^{fbr}*D* to different extent. These strains were constructed by replacing the original ribosome-binding site (RBS) in pED plasmid with one of four RBSs to generate B8/pED-RBS1, B8/pED-RBS2, B8/pED-RBS3, and B8/pED-RBS4 with different L-Trp productivities (the construction details can be found in supplementary materials). pSentrp was also introduced into each strain. We then measured the L-Trp-induced fluorescence (measured at 4 h after induction) and the extracellular L-Trp concentration, which were found to be positively correlated (Fig. 3) with an L-Trp-response range of 0.007–0.059 g/L/OD_{600} and 0.39–1.30 g/L for the extracellular and intracellular concentrations, respectively (measured after 24 h of fermentation). Moreover, the biosensor did not impact L-Trp biosynthesis *per se* because the extracellular L-Trp concentration was the same within experimental error when the strains did or did not contain pSentrp (Fig. S9). The aforementioned results strongly suggest that this biosensor can be used to reliably screen strains overproducing L-Trp.

3.2. Generation of the mutant library Trp-Push and screening for L-Trp-accumulating strains

With the biosensor in hand, we next looked to increase the availability of L-Trp by combinatorially modulating the upstream module. We, therefore, generated the Trp-Push library, and screened it for mutants producing L-Trp in substantial amounts using the L-Trp biosensor. With the triple knockout strain B8 (Δ*pheA*Δ*tnaA*Δ*tyrR*) constructed previously (Fang et al., 2015) as the parent strain, we looked for upregulation of *trpE*^{fbr}*D* (Gu et al., 2012; Zhao et al., 2011), *aroG*^{fbr}, (Berry, 1996) and *serA*^{fbr} (Rodrigues et al., 2013) as these genes substantially impact L-Trp synthesis (Fig. 4a). For each gene, an RBS library contained RBS sequences with the known theoretical translation initiation rates determined using an RBS calculator (Salis et al., 2009) was designed. These three genes together with their relevant RBS libraries were then assembled together and inserted into one acceptor vector pAC using OLMA method, (Fig. 4b), giving rise to the Trp-Push library (three-gene pathway with diverse expression strengths for each). 10 (*aroG*^{fbr} and *serA*^{fbr}) and 15 RBS (*trpE*^{fbr}*D*) sequences in each library were designed and constructed for the *trpE*^{fbr}*D*, *aroG*^{fbr}, and *serA*^{fbr} genes to cover protein expression levels of 2,873-, 52-, 248-fold based on the prediction of the RBS calculator (Table S2), thus leading to a theoretical library size of 1,500, which necessitates high-throughput screening. We also confirmed the reliability of the final library by sequencing 10 colonies after transformation. We found that 90% of the plasmids carried the designed pathway and had diverse RBS profiles, yielding >5000 colonies and representing a three-fold coverage for the designed library size.

The extracted plasmids from the Trp-Push library were co-transformed with pSentrp into B8 for high-throughput screening. The cells with the strongest fluorescence signals (top 2%) were retained, and then 24 colonies were subjected for further characterization. Most of them have sustainably enhanced tryptophan accumulation. Among them, three strains were found to be the best overproducer after flask fermentation confirmation, which was named after B8/pTrpH1, pTrpH2, and pTrp3, respectively. The L-Trp titers of the strains that did not carry pSentrp (removed by serial transfer into LB broth without ampicillin) were confirmed after flask cultivation, and their RBS profiles were determined by Sanger sequencing. Two of the strains B8/pTrpH1 and B8/pTrpH2 have the same genotype and L-Trp titers of 0.45 g/L, whereas the third strain B8/pTrpH3 exhibited a similar L-Trp titer of 0.44 g/L (the genotype for each strain is given in Table S3). Thus, by simultaneously modulating the three genes and subsequent FACS screening, we produced an ~100-fold increase in the L-Trp level in comparison with that of the parent strain B8/pAC (Fig. 4c).

We previously showed that an increase in L-Trp biosynthesis (upstream module) enhances violacein mixture (viocalein and deoxyviocalein) biosynthesis (similar to the downstream module in this work) (Fang et al., 2015). For this report, we inserted the downstream deoxyviolacein module (pDvio) into the parent strain (B8/pAC) and the optimized L-Trp overproducer B8/pTrpH1, respectively. B8/pTrpH1/pDvio has a 2.5-fold greater deoxyviolacein titer (0.19 g/L/OD_{600}) than does the parent strain B8/pAC/pDvio (0.08 g/L/OD_{600}; Fig. 4c). However, the increase in deoxyviolacein is less than expected at a 100-fold increase in L-Trp accumulation, indicating that a bottleneck existed in the downstream deoxyviolacein pathway.

3.3. Generation of the mutant library Vio-Pull and screening for a deoxyviolacein overproducer.

The deoxyviolacein pathway contains four enzymes, VioA, VioB, VioC, and VioE (Jiang et al., 2012; Rodrigues et al., 2013). VioB activity is rate-limiting for deoxyviolacein production given that when its copy number is increased, deoxyviolacein titers also increase substantially (unpublished data). However, because a sensor for deoxyviolacein does not exist so far, given the low throughput and the poor colour resolution when deoxyviolacein-producing colonies cultured on agar plates are screened (unpublished data), it has been very difficult to perform directed evolution to increase the activity of VioB. To overcome these problems, we used the negative high-throughput screening of the InterSPPS approach to increase deoxyviolacein biosynthesis. Briefly, we used the expected decrease in fluorescence reported by the L-Trp biosensor to screen for clones optimized for deoxyviolacein biosynthesis (i.e., the VioB bottleneck having been removed by protein engineering) given that L-Trp would be rapidly converted to deoxyviolacein when the downstream module is operating efficiently (Fig. 1a, Fig. S1).

We first assessed if this negative signal-based screening model would work as designed. The original pDvio plasmid carries two T7 promoters and one copy of the deoxyviolacein synthesis pathway under the control of one of the T7 promoters. Three plasmids containing an additional copy of *vioB*, *vioC*, or *vioE* under the control of the remaining T7 promoter (pDvio-vioB, pDvio-vioC, and pDvio-vioE, respectively) were constructed (the construction details of these three plasmids can be found in supplementary materials), and the plasmids were individually co-transformed with pSentrp into B8/pTrpH1 to mimic diverse downstream pathway carbon fluxes. We

found that the strains with the greater deoxyviolacein titers exhibited as expected decreased fluorescence and showed also less L-Trp accumulation (Fig. 5).

Having established the screening method to search for rate-limiting enzyme VioB mutants, we sought to further increase the activity of this enzyme. Knowing that overexpression of many genes under the control of strong promoters (i.e., in this case, *vioB* and other pathway genes are driven by T7 promoter) increases the metabolic burden of the host cell (Ajikumar et al., 2010), we suspected that using even stronger promoter or RBS engineering might limit the improvement space of this microbial cell factory. Hence, directed evolution is applied here aiming at increasing VioB activity rather than expression modulation. The *vioB* gene was amplified by error-prone PCR, and the products were assembled together with wild type *vioACE* genes into one pRSFDuet vector by OLMA method to generate the Vio-Pull library (20,000 colonies). The plasmids from this library were co-transformed with pSentrp into B8/pTrpH1 and then FACS screened. Strains were sorted into three groups based on their relative fluorescence, and two strains were randomly selected from each group. Strains L-1 and L-2 with relatively low fluorescence intensity have the same mutations in *vioB* and a relatively greater deoxyviolacein titer of 0.35 g/L/OD_{600}, which is 1.8-fold greater compared with that of the parent strain B8/pTrpH1/pDvio (0.19 g/L/OD_{600}; $P = 0.0004$ compared with the parent strain; Fig. 6a). Strains M1 and M2 with intermediate relative fluorescence also had the same genotype (but different to that of L series), and deoxyviolacein titers of 0.08 g/L/OD_{600}. Strains H1 and H2 with the highest relative fluorescence did not have the same mutations, and had relatively lower deoxyviolacein productivities accompanied by the greater fluorescence. The VioB mutations in these strains are listed in Fig. 6b.

3.4. Fermentation kinetics of B8/pTrpH1/pDVio-L1 in a 5-L bioreactor.

The fed-batch productivity of B8/pTrpH1/pDVio-L1 was assessed using a 5-L bioreactor with online control of pH and dissolved O_2 (Fig. S10). The time course profiles for glucose concentration, deoxyviolacein accumulation, and OD_{600} are shown in Fig. 7. Similar to our and other published reports on fed-batch fermentation to produce violacein (Fang et al., 2015; Rodrigues et al., 2013), deoxyviolacein accumulation also showed a growth-coupling pattern. Probably owing to growth inhibition caused by protein overexpression and deoxyviolacein biosynthesis, the final OD_{600} was only ~11, which is much smaller than that found for the conventional high-density fed-batch fermentation of *E. coli* (Zhao et al., 2013). Nonetheless, the final deoxyviolacein titer was 1.92 g/L at 48 h, which is a 20% improvement compared with the best recombinant *E. coli* that uses a simple carbon source (glycerol in that case) to produce deoxyviolacein (Rodrigues et al., 2014). More importantly, the productivity (40 mg/L/h) achieved with our *E. coli* construct present an improvement of five-fold compared with that achieved by Rodrigues *et al*. (Rodrigues et al., 2014). These comparisons indicate that InterSPPS is a practical, promising means by which to improve the performance of industrial microbial cell factories for production of natural metabolites.

4. Discussion

Rapid advances in synthetic biology have greatly improved combinatorial pathway library construction in terms of the genotypic space surveyed and library quality (Engler et al., 2009; Wang et al., 2009). However, the same cannot be said for high-throughput screening of phenotype space used during microbial cell factory

construction. Despite the potential of biosensors to fill this gap, poor knowledge of secondary metabolic pathway regulation (Cipriano et al., 2013) and protein sequence-structure-function relationships (Raman et al., 2014b) limit our ability to develop biosensors for many molecules of commercial interest, especially those associated with secondary metabolic pathways. Such recognition is evidenced by our search on June 26, 2015 of RegTransBase (Cipriano et al., 2013), a transcription regulation database based on literature mining. Notably, we found 266 transcription factors for amino acids effectors, 676 for carbohydrates, but only 5 for coenzymes and 187 for heterocyclic compounds (corresponding to 63 heterocyclic effectors as some of the transcription factors share the same effector). Our InterSPPS strategy provides a versatile platform to address this deficiency by making full use of a biosensor responsible for a compound residing at main metabolism junctions that can be used in a sequential push-pull style. Notably, using our new biosensor we substantially increased the synthesis of L-Trp during the positive screening portion of InterSPPS (metabolic push) via construction of a combinatorial library overexpressing *trpE*^{fbr}*D*, *aroG*^{fbr}, and *serA*^{fbr}. By doing so, the L-Trp and deoxyviolacein titers were increased by 100- and 2.5-fold, respectively. Subsequently, during the negative-screening portion of InterSPPS (metabolic pull), by improving the downstream activity of the rate-limiting enzyme VioB via directed evolution, the deoxyviolacein titer was increased by an additional 1.7-fold. In the fed-batch fermentation, the deoxyviolacein titer was 1.92 g/L and the productivity 40 mg/L/h; both values are the greatest reported to date (Rodrigues et al., 2014). Because deoxyviolacein has important antibacterial and antifungal activities (Jiang et al., 2012; Wang et al., 2012), our work provides an attractive means to produce this value-added natural product from glucose.

The success of InterSPPS largely depends on the properties of biosensor. For this report, we developed a biosensor with high specificity (Fig. S8b), good linear detection range, and a relatively intermediate dynamic range (Fig. 2b) that still proved effective during the optimization. However, further engineering efforts to increase the deoxyviolacein titer and productivity will rely on optimization of the biosensor. Its dynamic range is only eight-fold (Fig. 2b), which is smaller than some of other biosensors that have been successfully used in metabolic engineering applications (DeLoache et al., 2015; Raman et al., 2014a; Tang and Cirino, 2011). This limited dynamic range may hinder identification of clones that have moderate productivity differences. Concurrently, because the design of an InterSPPS biosensor needs a bi-directional screening ability, the upper and lower limits of the detection range need careful optimization. Specifically, the L-Trp biosensor has a linear detection range between 0.01 and 0.06 extracellular L-Trp/L/OD_{600} (Fig. 3), which is suboptimal for positive and negative screening of the two optimal modules. The limited dynamic range of the L-Trp biosensor might be circumvented by a variety of approaches. For example, mutation of a relevant site in *tnaC* or 23S RNA decreases the sensitivity of leader peptide retention to L-Trp (Martínez et al., 2014), which may, in turn, extend the detection range. In addition, we observed while using the biosensor to characterize endogenous L-Trp accumulation (Fig. 3) that the intracellular L-Trp concentration was ~10-fold greater than the extracellular concentration (data not shown). The intracellular L-Trp concentration may, therefore, have quickly saturated the biosensor capacity, thus limiting it upper detection limit. To address this problem, transporter engineering (Kind et al., 2014) might be incorporated during the positive screening phase so as to reduce the intracellular L-Trp concentration, thus allowing for better optimization of the upstream pathway.

Many enzymes in secondary metabolic pathways have only moderate activity compared with those involved in the central carbon metabolism, as suggested by database mining (Bar-Even and Salah Tawfik, 2013; Bar-Even et al., 2011) and practical examples (Brown et al., 2015; Xie et al., 2015), which hinders efforts to overproduce secondary metabolites. Given these observations, directed evolution is necessary to eliminate the protein-related bottlenecks. However, the lack of efficient screening methods greatly hinders such approaches. Herein, we have shown that InterSPPS provides a possible solution to this problem as evidenced by its ability to screen for a mutant (>20,000 clones) with improved activity for the rate-limiting enzyme VioB in the deoxyviolacein biosynthetic pathway. Unfortunately, owing to the lack of structure data and the difficulty of purifying VioB (unpublished data), we are not yet able to characterize the detailed mechanism underlying the effects of the mutations. However, our results clearly demonstrate the feasibility of using InterSPPS-assisted protein engineering to improve the enzymatic step(s) that is a bottleneck(s) in a secondary metabolic pathway. This approach could be applied to other secondary metabolic pathways that also have an enzyme(s) that substantially limits the production of an end product.

For biosynthetic pathways such as that for L-Trp, which is complex and tightly interconnected with core carbon metabolism (Rodrigues et al., 2013), it is especially important to highlight the necessity to simultaneously modulate the activities of different modules, because the effects of individual genetic manipulations are rarely additive (Ajikumar et al., 2010). High-throughput screening will thus be required, and biosensor is one of the most promising approaches to fulfill such requirements (Dietrich et al., 2010). In this context, a particularly vexing issue is the lack of biosensors that target many value-added secondary metabolic pathway products. As a

versatile platform, InterSPPS opens a new means for high-throughput screening that focuses on many secondary metabolic pathways. For example, using a constructed biosensor responding to malonyl-CoA (Li et al., 2015; Liu et al., 2015; Xu et al., 2014a, 2014b), L-Tyr (Chou and Keasling, 2013), L-Lys (Binder et al., 2012), L-Trp (this work), or isopentenyl pyrophosphate (Chou and Keasling, 2013), InterSPPS can enhance the biosynthesis of fatty acid(s) for use in biofuels (Guo et al., 2014) (from malonyl-CoA), isoquinoline alkaloids such as (*S*)-reticuline (DeLoache et al., 2015) (from L-Tyr), the biopolymer building block cadaverine (Kind et al., 2014) (from L-Lys), serotonin (from L-Trp) (Lin et al., 2014b), or terpenoids (Zhao et al., 2013) (from isopentenyl pyrophosphate), respectively. Additionally, a system of two InterSPPS-related biosensors can be easily modified to assist engineering of pathways having a branched architecture such as flavonoid biosynthesis, e.g., naringenin (Raman et al., 2014a) (L-Tyr and malonyl-CoA biosensors), or indole alkaloid biosynthesis, e.g., strictosidine (Brown et al., 2015) (L-Trp and isopentenyl pyrophosphate biosensors). Such combinations should substantially accelerate optimization processes by simultaneously monitoring multiple intermediate concentrations and quickly identifying the next targeted module, a module for which substrate (pathway intermediate) has accumulated. Such processes are quite labour intensive and inefficient during screen-free pathway engineering, owing to the substantially larger library size and metabolic landscape complexity.

5. Conclusion

To summarize, with the L-Trp biosensor developed in this work, InterSPPS strategy was applied to deoxyviolacein biosynthetic pathway as a proof of concept, by which the pathway was sequentially optimized in high-throughput manner without incorporating an end-product biosensor. This strategy successfully boosted the deoxyviolacein production to the titer of 1.92g/L, the highest level reported ever. In general, InterSPPS represents a powerful means to overproduce value-added natural products by pathway engineering and is expected to increase the efficiency and speed of microbial cell factory optimization processes in the future. This scheme should be especially helpful when optimizing secondary metabolic pathways for which biosensors for the target products have not been developed in many cases.

Acknowledgements

We thanked Dr. Tong Zhao from Flow Cytometry Facility, Institute of Mircobiology, Chinese Academy of Science, for assistance with flow cytometry and FACS. This work was supported by National Natural Science Foundation of China (NSFC 21376137) and Tsinghua University Initiative Scientific Research Program (2013Z02-1).

References

Ajikumar, P.K., Xiao, W.-H., Tyo, K.E.J., Wang, Y., Simeon, F., Leonard, E., Mucha, O., Phon, T.H., Pfeifer, B., Stephanopoulos, G., 2010. Isoprenoid pathway optimization for Taxol precursor overproduction in Escherichia coli. Science 330, 70–4. doi:10.1126/science.1191652

Atsumi, S., Hanai, T., Liao, J.C., 2008. Non-fermentative pathways for synthesis of branched-chain higher alcohols as biofuels. Nature 451, 86–9. doi:10.1038/nature06450

Bar-Even, A., Noor, E., Savir, Y., Liebermeister, W., Davidi, D., Tawfik, D.S., Milo, R., 2011. The moderately efficient enzyme: Evolutionary and physicochemical trends shaping enzyme parameters. Biochemistry 50, 4402–4410. doi:10.1021/bi2002289

Bar-Even, A., Salah Tawfik, D., 2013. Engineering specialized metabolic pathways--is there a room for enzyme improvements? Curr. Opin. Biotechnol. 24, 310–9. doi:10.1016/j.copbio.2012.10.006

Berry, A., 1996. Improving production of aromatic compounds in Escherichia coli by metabolic engineering. Trends Biotechnol. 14, 250–6. doi:10.1016/0167-7799(96)10033-0

Biggs, B.W., De Paepe, B., Santos, C.N.S., De Mey, M., Kumaran Ajikumar, P., 2014. Multivariate modular metabolic engineering for pathway and strain optimization. Curr. Opin. Biotechnol. 29, 156–62. doi:10.1016/j.copbio.2014.05.005

Binder, S., Schendzielorz, G., Stäbler, N., Krumbach, K., Hoffmann, K., Bott, M., Eggeling, L., 2012. A high-throughput approach to identify genomic variants of bacterial metabolite producers at the single-cell level. Genome Biol. 13, R40. doi:10.1186/gb-2012-13-5-r40

Binder, S., Siedler, S., Marienhagen, J., Bott, M., Eggeling, L., 2013. Recombineering in Corynebacterium glutamicum combined with optical nanosensors: a general strategy for fast producer strain generation. Nucleic Acids Res. 41, 6360–9. doi:10.1093/nar/gkt312

Brown, S., Clastre, M., Courdavault, V., O'Connor, S.E., 2015. De novo production of the plant-derived alkaloid strictosidine in yeast. Proc. Natl. Acad. Sci. U. S. A. 112, 3205–10. doi:10.1073/pnas.1423555112

Chen, W., Zhang, S., Jiang, P., Yao, J., He, Y., Chen, L., Gui, X., Dong, Z., Tang, S.-Y., 2015. Design of an ectoine-responsive AraC mutant and its application in metabolic engineering of ectoine biosynthesis. Metab. Eng. 30, 149–55. doi:10.1016/j.ymben.2015.05.004

Chen, Z., Rappert, S., Sun, J., Zeng, A.-P., 2011. Integrating molecular dynamics and co-evolutionary analysis for reliable target prediction and deregulation of the allosteric inhibition of aspartokinase for amino acid production. J. Biotechnol. 154, 248–54. doi:10.1016/j.jbiotec.2011.05.005

Cho, B.-K., Federowicz, S., Park, Y.-S., Zengler, K., Palsson, B.Ø., 2012. Deciphering the transcriptional regulatory logic of amino acid metabolism. Nat. Chem. Biol. 8, 65–71. doi:10.1038/nchembio.710

Chou, H.H., Keasling, J.D., 2013. Programming adaptive control to evolve increased metabolite production. Nat. Commun. 4, 2595. doi:10.1038/ncomms3595

Cipriano, M.J., Novichkov, P.N., Kazakov, A.E., Rodionov, D.A., Arkin, A.P., Gelfand, M.S., Dubchak, I., 2013. RegTransBase--a database of regulatory sequences and interactions based on literature: a resource for investigating transcriptional regulation in prokaryotes. BMC Genomics 14, 213. doi:10.1186/1471-2164-14-213

DeLoache, W.C., Russ, Z.N., Narcross, L., Gonzales, A.M., Martin, V.J.J., Dueber, J.E., 2015. An enzyme-coupled biosensor enables (S)-reticuline production in yeast from glucose. Nat. Chem. Biol. 11, 465–471. doi:10.1038/nchembio.1816

Dietrich, J. a, McKee, A.E., Keasling, J.D., 2010. High-throughput metabolic engineering: advances in small-molecule screening and selection., Annual review of biochemistry. doi:10.1146/annurev-biochem-062608-095938

Dietrich, J. a, Shis, D.L., Alikhani, A., Keasling, J.D., 2013. Transcription factor-based screens and synthetic selections for microbial small-molecule biosynthesis. ACS Synth. Biol. 2, 47–58. doi:10.1021/sb300091d

Engler, C., Gruetzner, R., Kandzia, R., Marillonnet, S., 2009. Golden gate shuffling: a one-pot DNA shuffling method based on type IIs restriction enzymes. PLoS One 4, e5553. doi:10.1371/journal.pone.0005553

Fang, M.-Y., Zhang, C., Yang, S., Cui, J.-Y., Jiang, P.-X., Lou, K., Wachi, M., Xing, X.-H., 2015. High crude violacein production from glucose by Escherichia coli engineered with interactive control of tryptophan pathway and violacein biosynthetic pathway. Microb. Cell Fact. 14, 8. doi:10.1186/s12934-015-0192-x

Gong, F., Yanofsky, C., 2002. Instruction of translating ribosome by nascent peptide. Science 297, 1864–7. doi:10.1126/science.1073997

Gong, F., Yanofsky, C., 2001. Reproducing tna operon regulation in vitro in an S-30 system. Tryptophan induction inhibits cleavage of TnaC peptidyl-tRNA. J. Biol. Chem. 276, 1974–83. doi:10.1074/jbc.M008892200

Gu, P., Yang, F., Kang, J., Wang, Q., Qi, Q., 2012. One-step of tryptophan attenuator inactivation and promoter swapping to improve the production of L-tryptophan in Escherichia coli. Microb. Cell Fact. 11, 30. doi:10.1186/1475-2859-11-30

Guo, D., Zhu, J., Deng, Z., Liu, T., 2014. Metabolic engineering of Escherichia coli for production of fatty acid short-chain esters through combination of the fatty acid and 2-keto acid pathways. Metab. Eng. 22, 69–75. doi:10.1016/j.ymben.2014.01.003

Jiang, P., Wang, H., Xiao, S., Fang, M., Zhang, R., He, S., Lou, K., Xing, X.-H., 2012. Pathway redesign for deoxyviolacein biosynthesis in Citrobacter freundii and characterization of this pigment. Appl. Microbiol. Biotechnol. 94, 1521–32. doi:10.1007/s00253-012-3960-0

Jiang, P., Wang, H., Zhang, C., Lou, K., Xing, X.-H., 2010. Reconstruction of the violacein biosynthetic pathway from Duganella sp. B2 in different heterologous hosts. Appl. Microbiol. Biotechnol. 86, 1077–88. doi:10.1007/s00253-009-2375-z

Jiang, W., Bikard, D., Cox, D., Zhang, F., Marraffini, L. a, 2013. RNA-guided editing of bacterial genomes using CRISPR-Cas systems. Nat. Biotechnol. 31, 233–9. doi:10.1038/nbt.2508

Jones, J.A., Toparlak, Ö.D., Koffas, M.A., 2015. Metabolic pathway balancing and its role in the production of biofuels and chemicals. Curr. Opin. Biotechnol. 33, 52–59. doi:10.1016/j.copbio.2014.11.013

Kikuchi, Y., Tsujimoto, K., Kurahashi, O., 1997. Mutational analysis of the feedback sites of phenylalanine-sensitive 3-deoxy-D-arabino-heptulosonate-7-phosphate synthase of Escherichia coli. Appl. Environ. Microbiol. 63, 761–2.

Kind, S., Neubauer, S., Becker, J., Yamamoto, M., Völkert, M., Abendroth, G. von, Zelder, O., Wittmann, C., 2014. From zero to hero - Production of bio-based nylon from renewable resources using engineered Corynebacterium glutamicum. Metab. Eng. 25, 113–123. doi:10.1016/j.ymben.2014.05.007

Klingenberg, M., Praff, E., 1967. Means of terminating reactions. Spec. assays Tech. 680–684.

Lee, M.E., Aswani, A., Han, A.S., Tomlin, C.J., Dueber, J.E., 2013. Expression-level optimization of a multi-enzyme pathway in the absence of a high-throughput assay. Nucleic Acids Res. 41, 10668–78. doi:10.1093/nar/gkt809

Li, S., Si, T., Wang, M., Zhao, H., 2015. Development of a Synthetic Malonyl-CoA Sensor in Saccharomyces cerevisiae for Intracellular Metabolite Monitoring and Genetic Screening. ACS Synth. Biol. doi:10.1021/acssynbio.5b00069

Lin, Y., Sun, X., Yuan, Q., Yan, Y., 2014a. Extending shikimate pathway for the production of muconic acid and its precursor salicylic acid in Escherichia coli. Metab. Eng. 23, 62–9. doi:10.1016/j.ymben.2014.02.009

Lin, Y., Sun, X., Yuan, Q., Yan, Y., 2014b. Engineering bacterial phenylalanine 4-hydroxylase for microbial synthesis of human neurotransmitter precursor 5-hydroxytryptophan. ACS Synth. Biol. 3, 497–505. doi:10.1021/sb5002505

Liu, C.C., Qi, L., Yanofsky, C., Arkin, A.P., 2011. Regulation of transcription by unnatural amino acids. Nat. Biotechnol. 29, 164–8. doi:10.1038/nbt.1741

Liu, D., Xiao, Y., Evans, B.S., Zhang, F., 2015. Negative feedback regulation of fatty acid production based on a malonyl-CoA sensor-actuator. ACS Synth. Biol. 4, 132–40. doi:10.1021/sb400158w

Martínez, A.K., Gordon, E., Sengupta, A., Shirole, N., Klepacki, D., Martinez-Garriga, B., Brown, L.M., Benedik, M.J., Yanofsky, C., Mankin, A.S., Vazquez-Laslop, N., Sachs, M.S., Cruz-Vera, L.R., 2014. Interactions of the TnaC nascent peptide with rRNA in the exit tunnel enable the ribosome to respond to free tryptophan. Nucleic Acids Res. 42, 1245–56. doi:10.1093/nar/gkt923

Miller, G.L., 1959. Use of Dinitrosalicylic Acid Reagent for Determination of Reducing Sugar. Anal. Chem. 31, 426–428. doi:10.1021/ac60147a030

Mustafi, N., Grünberger, A., Kohlheyer, D., Bott, M., Frunzke, J., 2012. The development and application of a single-cell biosensor for the detection of l-methionine and branched-chain amino acids. Metab. Eng. 14, 449–57. doi:10.1016/j.ymben.2012.02.002

Mustafi, N., Grünberger, A., Mahr, R., Helfrich, S., Nöh, K., Blombach, B., Kohlheyer, D., Frunzke, J., 2014. Application of a genetically encoded biosensor for live cell imaging of L-valine production in pyruvate dehydrogenase complex-deficient Corynebacterium glutamicum strains. PLoS One 9, e85731. doi:10.1371/journal.pone.0085731

Neidhardt, F.C., Bloch, P.L., Smith, D.F., 1974. Culture medium for enterobacteria. J. Bacteriol. 119, 736–47.

Paddon, C.J., Westfall, P.J., Pitera, D.J., Benjamin, K., Fisher, K., McPhee, D., Leavell, M.D., Tai, a, Main, a, Eng, D., Polichuk, D.R., Teoh, K.H., Reed, D.W., Treynor, T., Lenihan, J., Fleck, M., Bajad, S., Dang, G., Dengrove, D., Diola, D., Dorin, G., Ellens, K.W., Fickes, S., Galazzo, J., Gaucher, S.P., Geistlinger, T., Henry, R., Hepp, M., Horning, T., Iqbal, T., Jiang, H., Kizer, L., Lieu, B., Melis, D., Moss, N., Regentin, R., Secrest, S., Tsuruta, H., Vazquez, R., Westblade, L.F., Xu, L., Yu, M., Zhang, Y., Zhao, L., Lievense, J., Covello, P.S., Keasling, J.D., Reiling, K.K., Renninger, N.S., Newman, J.D., 2013. High-level semi-synthetic production of the potent antimalarial artemisinin. Nature 496, 528–32. doi:10.1038/nature12051

Raman, S., Rogers, J.K., Taylor, N.D., Church, G.M., 2014a. Evolution-guided optimization of biosynthetic pathways. Proc. Natl. Acad. Sci. 111, 201409523. doi:10.1073/pnas.1409523111

Raman, S., Taylor, N., Genuth, N., Fields, S., Church, G.M., 2014b. Engineering allostery. Trends Genet. 30, 521–528. doi:10.1016/j.tig.2014.09.004

Ro, D.-K., Paradise, E.M., Ouellet, M., Fisher, K.J., Newman, K.L., Ndungu, J.M., Ho, K.A., Eachus, R.A., Ham, T.S., Kirby, J., Chang, M.C.Y., Withers, S.T., Shiba, Y., Sarpong, R., Keasling, J.D., 2006. Production of the antimalarial drug precursor artemisinic acid in engineered yeast. Nature 440, 940–3. doi:10.1038/nature04640

Rodrigues, A.L., Becker, J., de Souza Lima, A.O., Porto, L.M., Wittmann, C., 2014. Systems metabolic engineering of Escherichia coli for gram scale production of the antitumor drug deoxyviolacein from glycerol. Biotechnol. Bioeng. 111, 2280–9. doi:10.1002/bit.25297

Rodrigues, A.L., Trachtmann, N., Becker, J., Lohanatha, A.F., Blotenberg, J., Bolten, C.J., Korneli, C., de Souza Lima, A.O., Porto, L.M., Sprenger, G.A., Wittmann, C., 2013. Systems metabolic engineering of Escherichia coli for production of the antitumor drugs violacein and deoxyviolacein. Metab. Eng. 20, 29–41. doi:10.1016/j.ymben.2013.08.004

Salis, H.M., Mirsky, E.A., Voigt, C.A., 2009. Automated design of synthetic ribosome binding sites to control protein expression. Nat. Biotechnol. 27, 946–50. doi:10.1038/nbt.1568

Schendzielorz, G., Dippong, M., Grünberger, A., Kohlheyer, D., Yoshida, A., Binder, S., Nishiyama, C., Nishiyama, M., Bott, M., Eggeling, L., 2014. Taking control over control: use of product sensing in single cells to remove flux control at key enzymes in biosynthesis pathways. ACS Synth. Biol. 3, 21–9. doi:10.1021/sb400059y

Siedler, S., Stahlhut, S.G., Malla, S., Maury, J., Neves, A.R., 2014. Novel biosensors based on flavonoid-responsive transcriptional regulators introduced into Escherichia coli. Metab. Eng. 21, 2–8. doi:10.1016/j.ymben.2013.10.011

Spraggon, G., Kim, C., Nguyen-Huu, X., Yee, M.C., Yanofsky, C., Mills, S.E., 2001. The structures of anthranilate synthase of Serratia marcescens crystallized in the presence of (i) its substrates, chorismate and glutamine, and a product, glutamate, and (ii) its end-product inhibitor, L-tryptophan. Proc. Natl. Acad. Sci. U. S. A. 98, 6021–6. doi:10.1073/pnas.111150298

Tang, S.-Y., Cirino, P.C., 2011. Design and application of a mevalonate-responsive regulatory protein. Angew. Chem. Int. Ed. Engl. 50, 1084–6. doi:10.1002/anie.201006083

Tang, S.-Y., Fazelinia, H., Cirino, P.C., 2008. AraC regulatory protein mutants with altered effector specificity. J. Am. Chem. Soc. 130, 5267–71. doi:10.1021/ja7109053

Tang, S.-Y., Qian, S., Akinterinwa, O., Frei, C.S., Gredell, J.A., Cirino, P.C., 2013. Screening for enhanced triacetic acid lactone production by recombinant Escherichia coli expressing a designed triacetic acid lactone reporter. J. Am. Chem. Soc. 135, 10099–103. doi:10.1021/ja402654z

Wang, H., Wang, F., Zhu, X., Yan, Y., Yu, X., Jiang, P., Xing, X.H., 2012. Biosynthesis and characterization of violacein, deoxyviolacein and oxyviolacein in heterologous host, and their antimicrobial activities. Biochem. Eng. J. 67, 148–155. doi:10.1016/j.bej.2012.06.005

Wang, H.H., Isaacs, F.J., Carr, P. a, Sun, Z.Z., Xu, G., Forest, C.R., Church, G.M., 2009. Programming cells by multiplex genome engineering and accelerated evolution. Nature 460, 894–8. doi:10.1038/nature08187

Wiedenheft, B., Sternberg, S.H., Doudna, J. a, 2012. RNA-guided genetic silencing systems in bacteria and archaea. Nature 482, 331–8. doi:10.1038/nature10886

Woolston, B.M., Edgar, S., Stephanopoulos, G., 2013. Metabolic engineering: past and future. Annu. Rev. Chem. Biomol. Eng. 4, 259–88. doi:10.1146/annurev-chembioeng-061312-103312

Wu, J., Du, G., Zhou, J., Chen, J., 2013. Metabolic engineering of Escherichia coli for (2S)-pinocembrin production from glucose by a modular metabolic strategy. Metab. Eng. 16, 48–55. doi:10.1016/j.ymben.2012.11.009

Xie, W., Lv, X., Ye, L., Zhou, P., Yu, H., 2015. Construction of lycopene-overproducing Saccharomyces cerevisiae by combining directed evolution and metabolic engineering. Metab. Eng. 30, 69–78. doi:10.1016/j.ymben.2015.04.009

Xu, P., Gu, Q., Wang, W., Wong, L., Bower, A.G.W., Collins, C.H., Koffas, M.A.G., 2013. Modular optimization of multi-gene pathways for fatty acids production in E. coli. Nat. Commun. 4, 1409. doi:10.1038/ncomms2425

Xu, P., Li, L., Zhang, F., Stephanopoulos, G., Koffas, M., 2014a. Improving fatty acids production by engineering dynamic pathway regulation and metabolic control. Proc. Natl. Acad. Sci. 111, 11299–11304. doi:10.1073/pnas.1406401111

Xu, P., Wang, W., Li, L., Bhan, N., Zhang, F., Koffas, M.A.G., 2014b. Design and kinetic analysis of a hybrid promoter-regulator system for malonyl-CoA sensing in Escherichia coli. ACS Chem. Biol. 9, 451–8. doi:10.1021/cb400623m

Yang, C., Jiang, P., Xiao, S., Zhang, C., Lou, K., Xing, X.-H., 2011. Fed-batch fermentation of recombinant Citrobacter freundii with expression of a violacein-synthesizing gene cluster for efficient violacein production from glycerol. Biochem. Eng. J. 57, 55–62. doi:10.1016/j.bej.2011.08.008

Yang, J., Seo, S.W., Jang, S., Shin, S.-I., Lim, C.H., Roh, T.-Y., Jung, G.Y., 2013. Synthetic RNA devices to expedite the evolution of metabolite-producing microbes. Nat. Commun. 4, 1413. doi:10.1038/ncomms2404

Yanofsky, C., Horn, V., Gollnick, P., 1991. Physiological studies of tryptophan transport and tryptophanase operon induction in Escherichia coli. J. Bacteriol. 173, 6009–17.

Ye, F., Kuang, Y., Chen, S., Zhang, C., Chen, Y., Xing, X.-H., 2009. Characteristics of low molecular weight heparin production by an ultrafiltration membrane bioreactor using maltose binding protein fused heparinase I. Biochem. Eng. J. 46, 193–198. doi:10.1016/j.bej.2009.05.007

Yuan, L.Z., Rouvière, P.E., Larossa, R.A., Suh, W., 2006. Chromosomal promoter replacement of the isoprenoid pathway for enhancing carotenoid production in E. coli. Metab. Eng. 8, 79–90. doi:10.1016/j.ymben.2005.08.005

Zelcbuch, L., Antonovsky, N., Bar-Even, A., Levin-Karp, A., Barenholz, U., Dayagi, M., Liebermeister, W., Flamholz, A., Noor, E., Amram, S., Brandis, A., Bareia, T., Yofe, I., Jubran, H., Milo, R., 2013. Spanning high-dimensional expression space using ribosome-binding site combinatorics. Nucleic Acids Res. 41, e98. doi:10.1093/nar/gkt151

Zhang, F., Ouellet, M., Batth, T.S., Adams, P.D., Petzold, C.J., Mukhopadhyay, A., Keasling, J.D., 2012. Enhancing fatty acid production by the expression of the regulatory transcription factor FadR. Metab. Eng. 14, 653–660. doi:10.1016/j.ymben.2012.08.009

Zhao, H., Moore, J.C., Volkov, A.A., Arnold, F.H., 1999. Methods for optimizing industrial enzymes by directed evolution. Man. Ind. Microbiol. Biotechnol. 597–604.

Zhao, J., Li, Q., Sun, T., Zhu, X., Xu, H., Tang, J., Zhang, X., Ma, Y., 2013. Engineering central metabolic modules of Escherichia coli for improving β-carotene production. Metab. Eng. 17, 42–50. doi:10.1016/j.ymben.2013.02.002

Zhao, Z.-J., Zou, C., Zhu, Y.-X., Dai, J., Chen, S., Wu, D., Wu, J., Chen, J., 2011. Development of L-tryptophan production strains by defined genetic modification in Escherichia coli. J. Ind. Microbiol. Biotechnol. 38, 1921–9. doi:10.1007/s10295-011-0978-8

Tables

Table. 1. List of strains used in this work

Strains or plasmids	Characteristics	Source
Strains		
B8	*E. coli* BL21(DE3) *ΔtrpRΔtnaAΔpheA*	Fang, M.-Y. et al.,
plasmids		
pAC	pACYCDuet, T7 promoter, Cm^R	Novogen
pRSF	pRSFDuet, T7 promoter, Km^R	Novogen
pED	pACYCDuet with $trpE^{fbr}D$ (Met293Thr, TCC to TTC; Ser40Leu ATG to ACG), Cm^R	Fang, M.-Y. et al.,
pComVioΔD	pCom10 carrying deoxyviolacein biosynthesis pathway, vioABEC, Km^R	Jiang, P., et al., 2012
pDvio	pRSFDuet with deoxyviolacein biosynthesis pathway, vioABEC, Km^R	This study
pSentrp	pTrc99A with regulatory element and eGFP, Amp^R	This study
pED-RBS1,2,3,4	The plasmids with RBS mutated from pED, Cm^R	This study
pHD	Backbone free of BsaI restriction site, Tet^R	Life Technology
pHD-trpED	pHD1 with $trpE^{fbr}D$, Tet^R	This study
pHD-serA	pHD1 with $serA^{fbr}$ (Thr327Asp, ACT to GAT), Tet^R	This study
pHD-aroG	pHD1 with $aroG^{fbr}$ (Asp146Asn, GAT to AAT; Pro150Leu, CCA to CTA), Tet^R	This study
Trp-PUSH library	pACYCDuet with $trpE^{fbr}D$, $serA^{fbr}$, $aroG^{fbr}$, all	This study

	RBSs were from libraries, Cm^R	
pTrpH1,2,3	The plasmids which were selected from Trp-PUSH library	This study
pDvio-vioB/vioC/vioE	pDvio carrying one additional copy of vioB, vioC, vioE driven by T7 promoter	This study
pHD-vioa	pHD1 with vioA, Tet^R	This study
pHD-viob	pHD1 with vioB (generated by error prone PCR), Tet^R	This study
pHD-vioce	pHD1 with vioCE, Tet^R	This study
Vio-PULL library	pRSFDuet with vioABCE, of which the vioB gene was a library generated by error prone PCR, Km^R	This study
pDvio-L1/2,M1/2,H1/2	The plasmids which were selected from Vio-PULL library	This study

Figure Captions

Fig. 1. Intermediate sensor–assisted push-pull strategy enables sequential pathway optimization (InterSPPS) in a high-throughput manner without using an end-product biosensor. (a) A generalized InterSPPS schematic. 1. When a biosensor (light bulb) targets an intermediate in a biosynthesis pathway, the pathway can be considered as two modules connected by the intermediate molecule. 2. The upstream module can be enhanced first by constructing a library containing mutants that produce more of the intermediate. High-throughput screening for such mutants is then performed using the biosensor as the monitor, with the expectation that the intensity of the biosensor will increase. 3. The activities of the components of the downstream module can then be optimized so that they readily use the intermediate produced by the upstream module. This step also relies on high-throughput screening using the intermediate biosensor as the monitor, with the expectation that the intensity of the biosensor will decrease due to the depletion of intermediate owing to the enhanced activity of the downstream module. The resulting pathway should then be overproducing the end product and its metabolic flux can well be balanced. (b) A schematic of the deoxyviolacein biosynthetic pathway with glucose as the initial carbon source and L-Trp as the defining intermediate (G6P: glucose 6-phosphate, FDP: fructose 1,6-biphosphate, DHAP: dihydroxyacetone phosphate, G3P: glyceraldehyde 3-phosphate, PEP: phosphoenolpyruvate, PYR: pyruvate, AcCoA: acetyl-CoA, CIT: citrate, MAL: malate, OAA: oxaloacetate, DAHP: 2-Dehydro-3-deoxy-D-arabino-heptonate 7-phosphate, CA: chorismate, TRP: L-Trp, dVIO: deoxyviolacein). The

final titers of L-Trp and deoxyviolacein and their relative production increases are shown in the upper right corner of the figure.

Fig. 2. Performance of the L-Trp biosensor in the presence of extracellular Ala-Trp. (a) Top panel, natural attenuation of *tnaCAB* expression occurs via ribosomal pausing of partially translated TnaC, the leader peptide of the *tnaCAB* operon at its terminal proline codon. In the absence of L-Trp, the TnaC leader peptide is released from the tRNA and the ribosome, which allows the Rho factor to access the Rho-dependent terminator on *tnaCAB* and prematurely terminate transcription. Bottom panel, in the presence of L-Trp, access by Rho is blocked and transcription of *tnaCAB* continues. Based on this mechanism, to construct the biosensor, we replaced *tnaAB* with *eGFP* so that the TnaC-based native-like regulatory device can be induced by intracellular L-Trp and the intracellular L-Trp concentration can be monitored as a fluorescent signal. (b) Response of the biosensor towards external Ala-Trp characterized by fluorescence spectrometry (green squares; RFU, relative fluorescence unit) and flow cytometry (orange circles; MFU, medium fluorescence unit). The fluorescence signal plateaued when the dipeptide concentration exceeded 1.5 mM even though more intracellular L-Trp accumulated at greater Ala-Trp concentrations (data not shown). Data in Fig. 2b are presented as the mean ± SD; n = 3.

Fig. 3. Dose-response by the biosensor in strains that accumulate L-Trp to different extents. The fluorescence signal was measured at 4 h after IPTG induction, and **L**-Trp accumulation was measured after a 24-h culture. Green bar: fluorescence signal determined by normalized RFU, Blue bar: extracellular L-Trp concentration. Data are presented as the mean ± SD; n = 3.

Fig. 4. Construction and screening of the Trp-Push library to increase the L-Trp and deoxyviolacein titers. (a) In the established strain B8 containing the triple knockout Δ*pheA*Δ*tnaA*Δ*trpR*, L-Trp biosynthesis was further strengthened by overexpressing three key enzymes, $TrpE^{fbr}D$, $AroG^{fbr}$, and $SerA^{fbr}$. The known feedback inhibition sites residing in the corresponding three wild-type enzymes had been eliminated by mutations as described in Materials and Methods (Section 2.5.). (b) The combinatorial library Trp-Push was constructed to modulate the expression of $TrpE^{fbr}D$, $AroG^{fbr}$, and $SerA^{fbr}$ via RBS engineering. A schematic of the OLMA method used to construct the Trp-Push library is shown. Between 10 and 15 RBSs with a wide range of translation strengths according to the RBS calculator predictions were designed for the three enzymes. The RBS sequences were ligated onto the structural genes by OLMA method and inserted into the acceptor vector pAC to generate the Trp-Push library that can simultaneously express the three genes with diverse strength. (c) L-Trp (blue bar) and deoxyviolacein (purple bar) accumulation for the best L-Trp producer (B8/pTrpH1) retrieved by FACS facilitated with biosensor monitoring and the parent strain (B8/pAC). For deoxyviolacein biosynthesis, pDvio was transformed into the optimized B8/TrpH1 and parent B8/pAC strains. Data are presented as the mean ± SD; n = 3. **, $P < 0.01$; ***, $P < 0.001$; two-tailed *t*-test.

Fig. 5. InterSPPS negative screening capability tested using B8/pTrpH1/pDvio-vioC, B8/pTrpH1/pDvio-vioE and B8/pTrpH1/pDvio-vioB with diverse deoxyviolacein biosynthetic activities. (a) Deoxyviolacein biosynthetic capacities of the three strains measured at 4 h after IPTG addition. (b) Relative biosensor fluorescence measured at 4 h after IPTG addition. The deoxyviolacein biosynthetic capacity of each strain (Fig. 5a) negatively correlates with the biosensor relative fluorescence signal. (**c**) Extracellular L-Trp concentration measured at 24 h after IPTG addition. The negative correlation between the fluorescence signal and deoxyviolacein accumulation probably is a consequence of L-Trp depletion. Data are presented as the mean ± SD; n = 3.

Fig. 6. Phenotypic and genotypic characterisation of strains retrieved by InterSPPS negative screening from the Vio-Pull library that contains the *vioB* mutant library created by error-prone PCR. (a) Six strains were isolated from the Vio-Pull library and categorised into three groups according to their biosensor fluorescence. L1/2, relatively little fluorescence; M1/2, intermediate fluorescence; and H1/2 relatively large fluorescence. Because the L1/2 pair has the same genotype as shown by Sanger sequencing, the flask fermentation data for the two clones were averaged. M1 and M2 also have the same genotype (although different from that of L1 and L2), and their data were also averaged. The fluorescence intensities and deoxyviolacein accumulations of these six strains (after removal of pSentrp) were measured as described in Methods. Data are presented as the mean ± SD; n = 6 for L1/2, and M1/2, and n = 3 for the H strains and the parent strain. ***, $P < 0.001$, two-tailed *t*-test was performed for the final deoxyviolacein titer of L1/2 and their parent strain. (b) Nucleotide mutations identified by Sanger sequencing and the corresponding amino acid mutations.

Fig. 7. Fed-batch fermentation of B8/pTrpH1/pDVio-L1 for deoxyviolacein production. The culture OD_{600}, residual glucose concentration, and deoxyviolacein titer were measured during a 60-h fermentation.

Highlights

- An L-Trp biosensor was developed based on native control of the tryptophanase operon.

- The deoxyviolacein pathway was divided into two modules, providing and utilizing Trp, respectively.

- The biosenor was used for screening combinatorial libraries of upstream module for increased L-Trp formation.

- Subsequently the same biosensor was used for screening downstream enzyme vioB mutant library based on reduced L-Trp-dependent biosensor output.

- With this biosensor-coupled push/pull approach, a strain accumulating 1.92 g/L deoxyviolacein in fed-batch fermentation was obtained.

Figure1

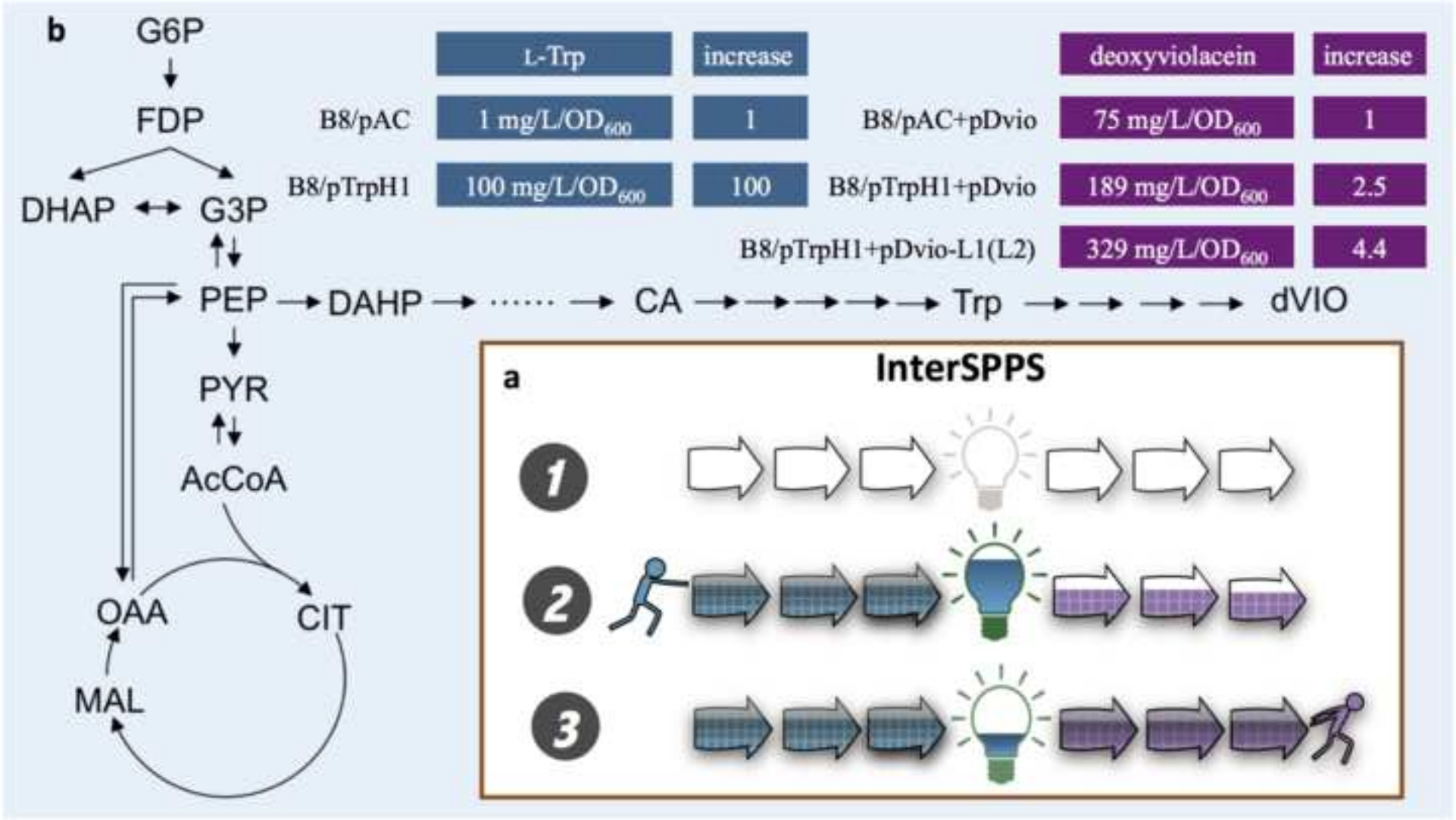

Figure2

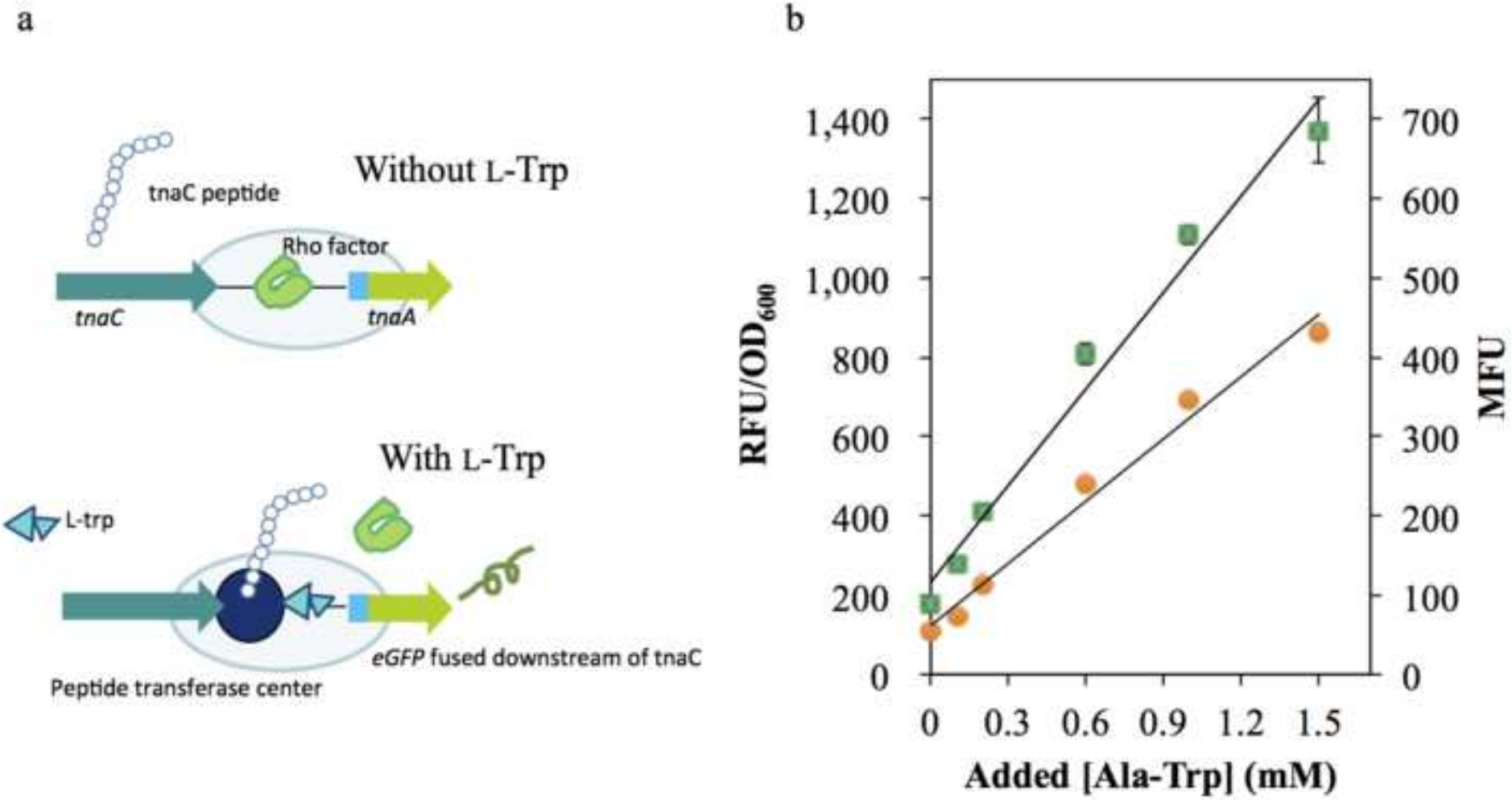

Figure3

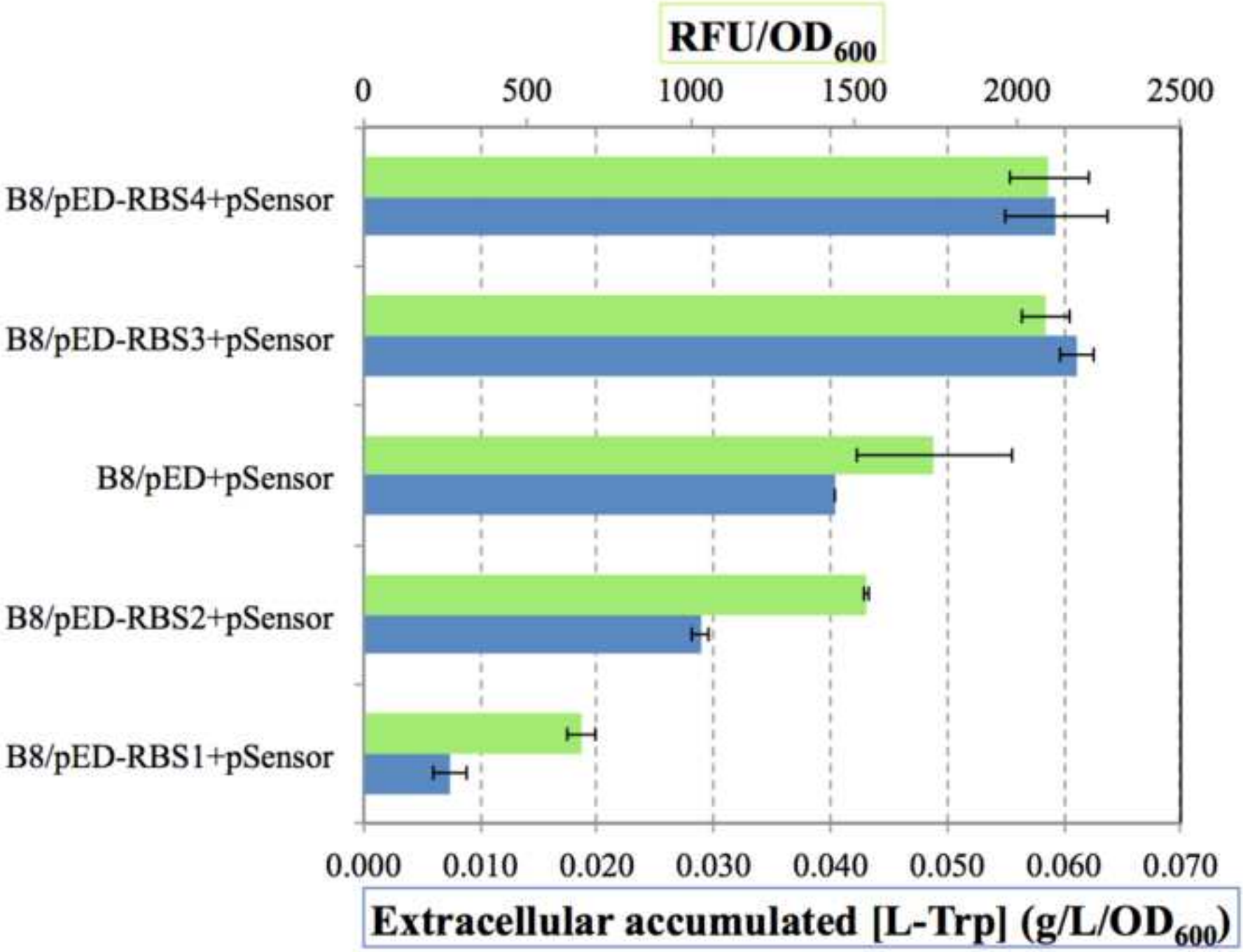

Figure4

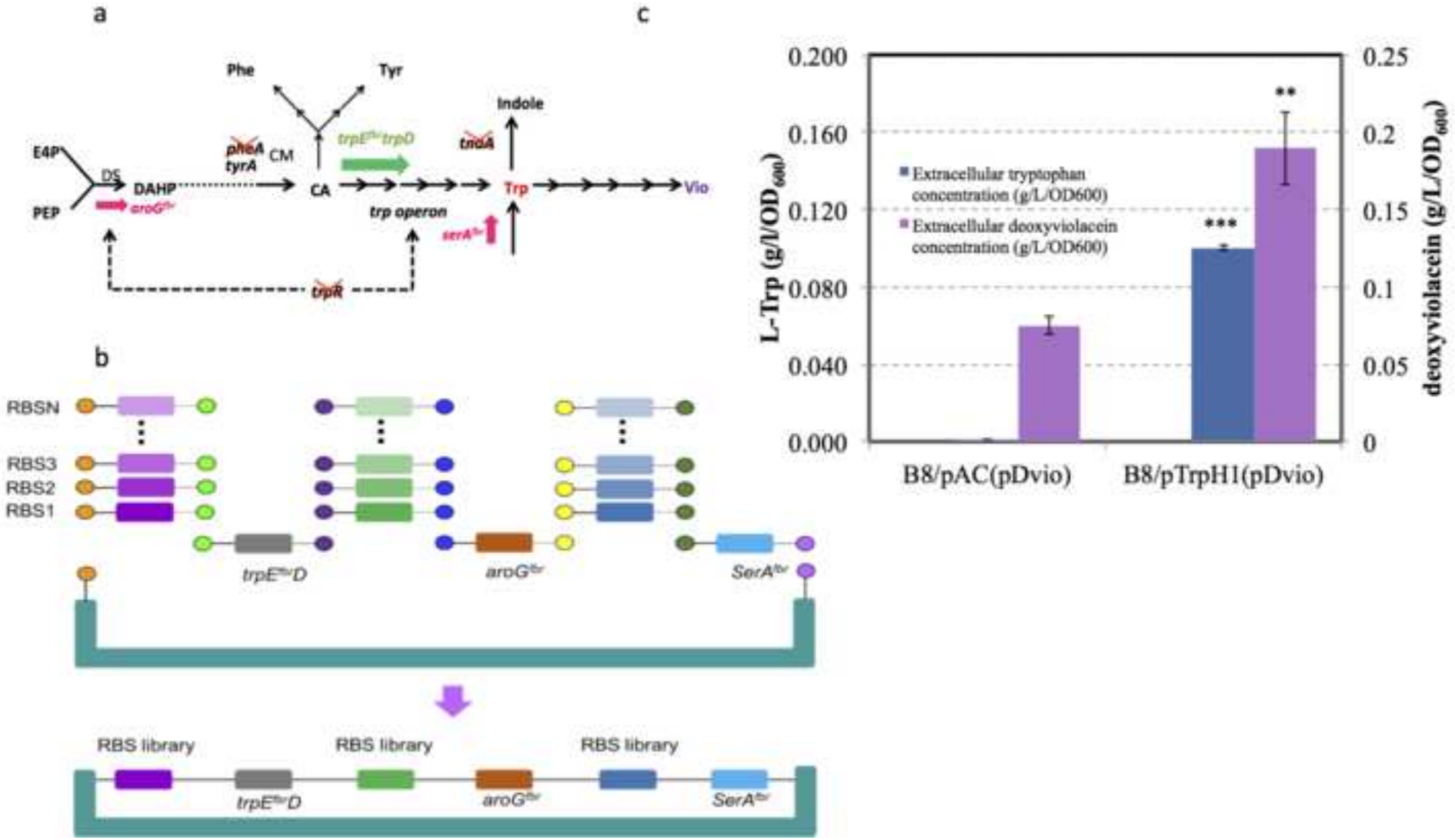

Figure5

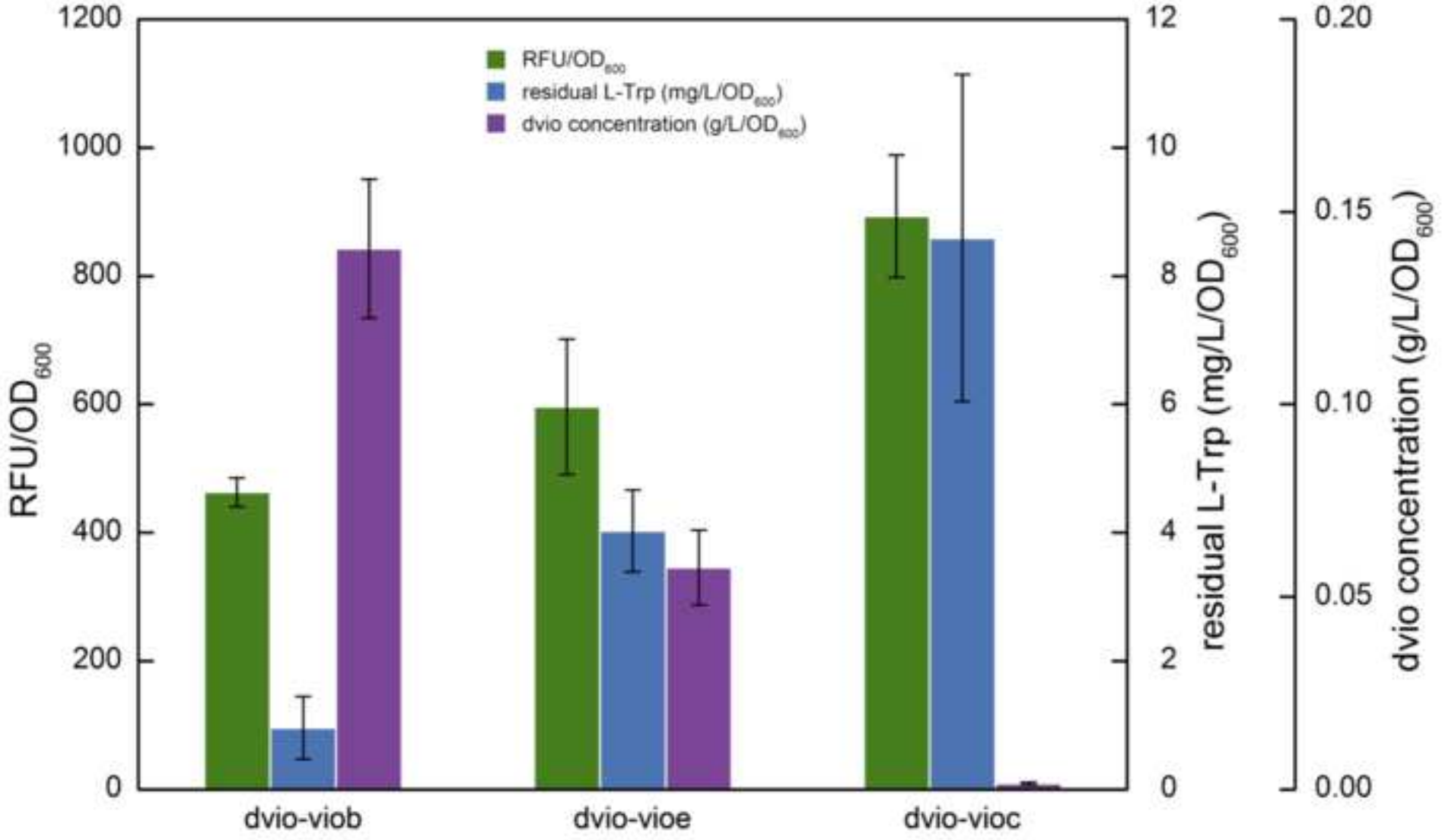

Figure6

a

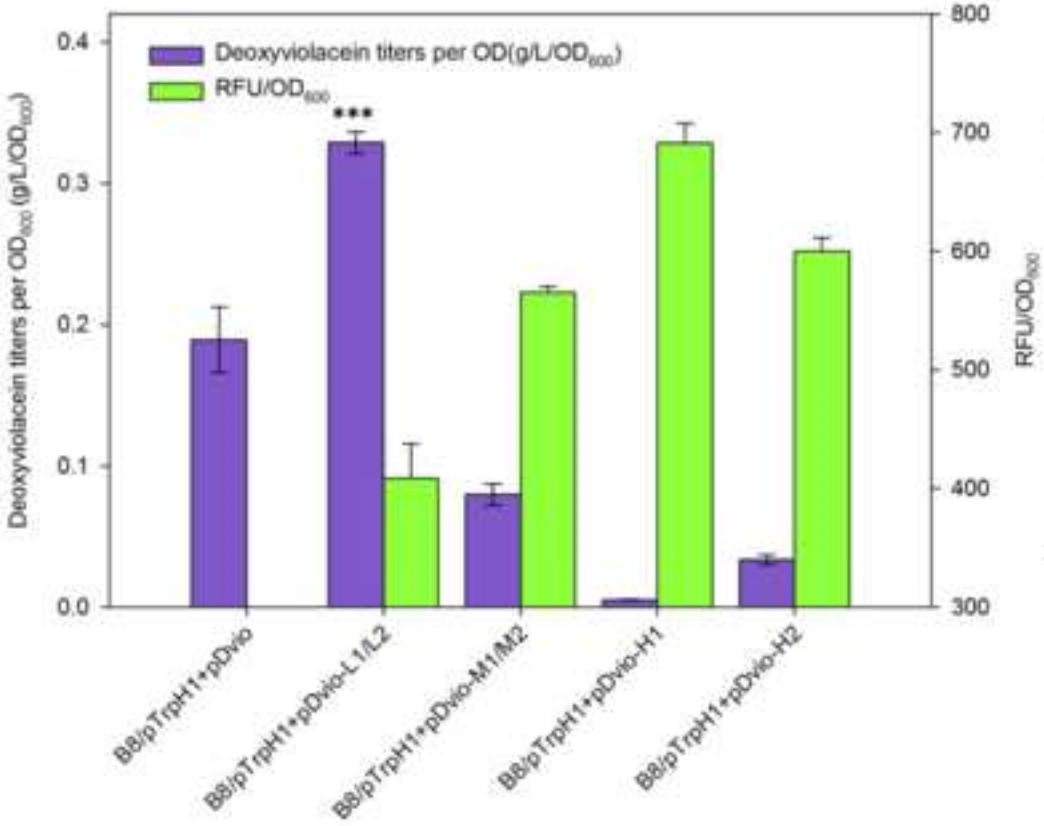

b

Plasmid	Nucleotide mutation	Amino acid mutation
pDvio-L1 (L2)	C414A, A610C, T616C, G1823T, C1118T, A6C, A1224G, C1822T, T1945C, T2258C, T2515G	Phe206Leu, Arg373Cys, Arg2Ser, Pro608Leu, Val753Ala, Ser839Ala
pDvio-M1 (M2)	T2515G,A134G	Ser839Ala,asp45Gly
pDvio-H1	A174G, T264C, A461G, T858C, C895T, T1013C, G1040A, T1104A, C2752A, A2776T, C1118T, T2258C, T2515G	Gln154Arg, Leu338Pro, Gly347Asp, His368Gln, Asn926Tyr, Arg373Cys, Val753Ala, Ser839Ala
pDvio-H2	T463A, G636A, A1422G, A1422G, T2248A, A2804G, T2515G	Phe155Ile, Phe750Ile, Asn935Ser, Ser839Ala

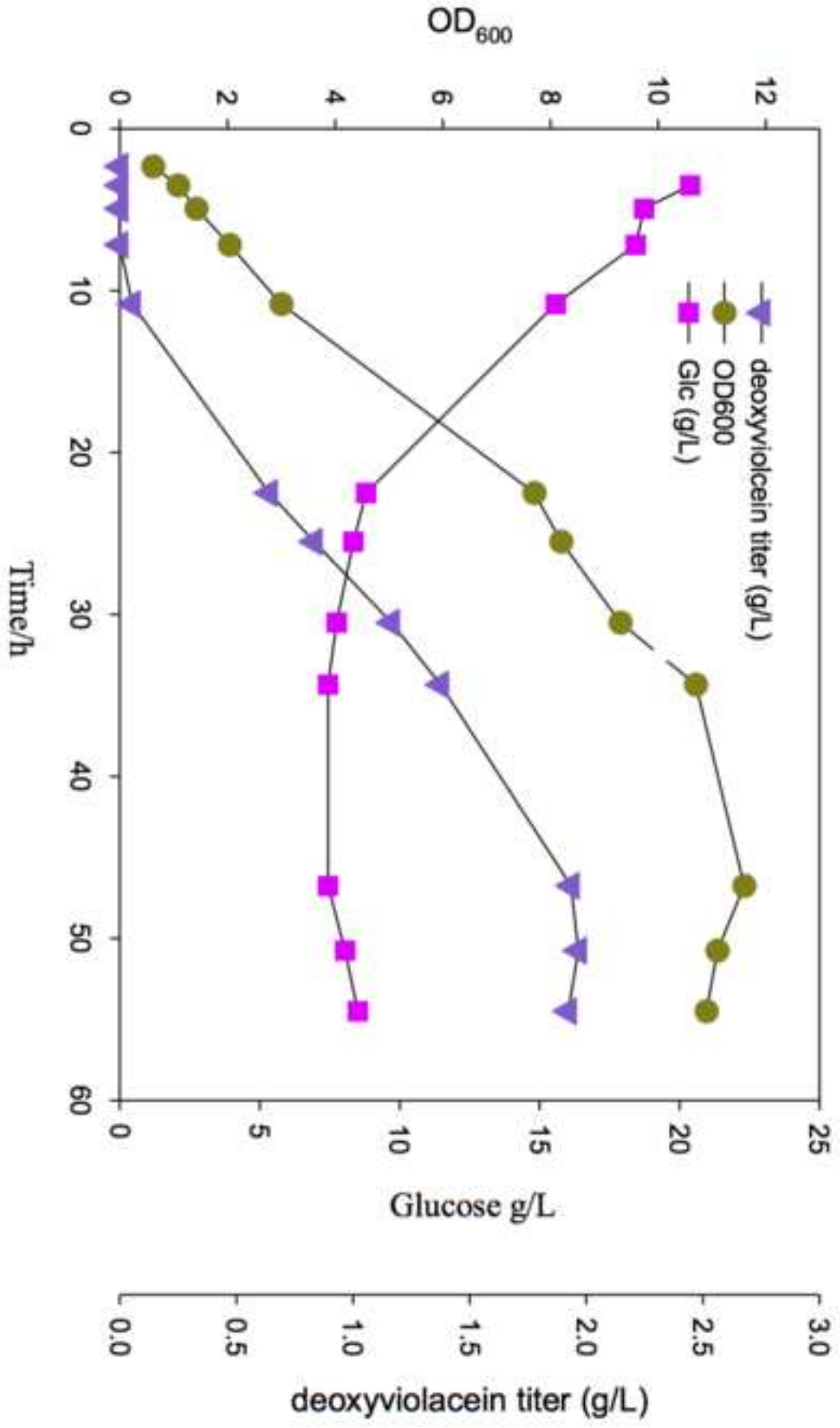
OD600
0
2
4
6
8
10
12
Time/h
0
10
20
30
40
50
60
deoxyviolcein titer (g/L)
OD600
Glc (g/L)
Glucose g/L
0
5
10
15
20
25
deoxyviolacein titer (g/L)
0.0
0.5
1.0
1.5
2.0
2.5
3.0

Figure7